

Introduction

- Globally connected multidecadal climate variations (MCV) are observed on top of non-uniform global warming trend (Deser and Phillips 2017; Kravtsov et al. 2018)
- This signal may represent **internal variability** or reflect **complex teleconnectivity of the forced climate response**

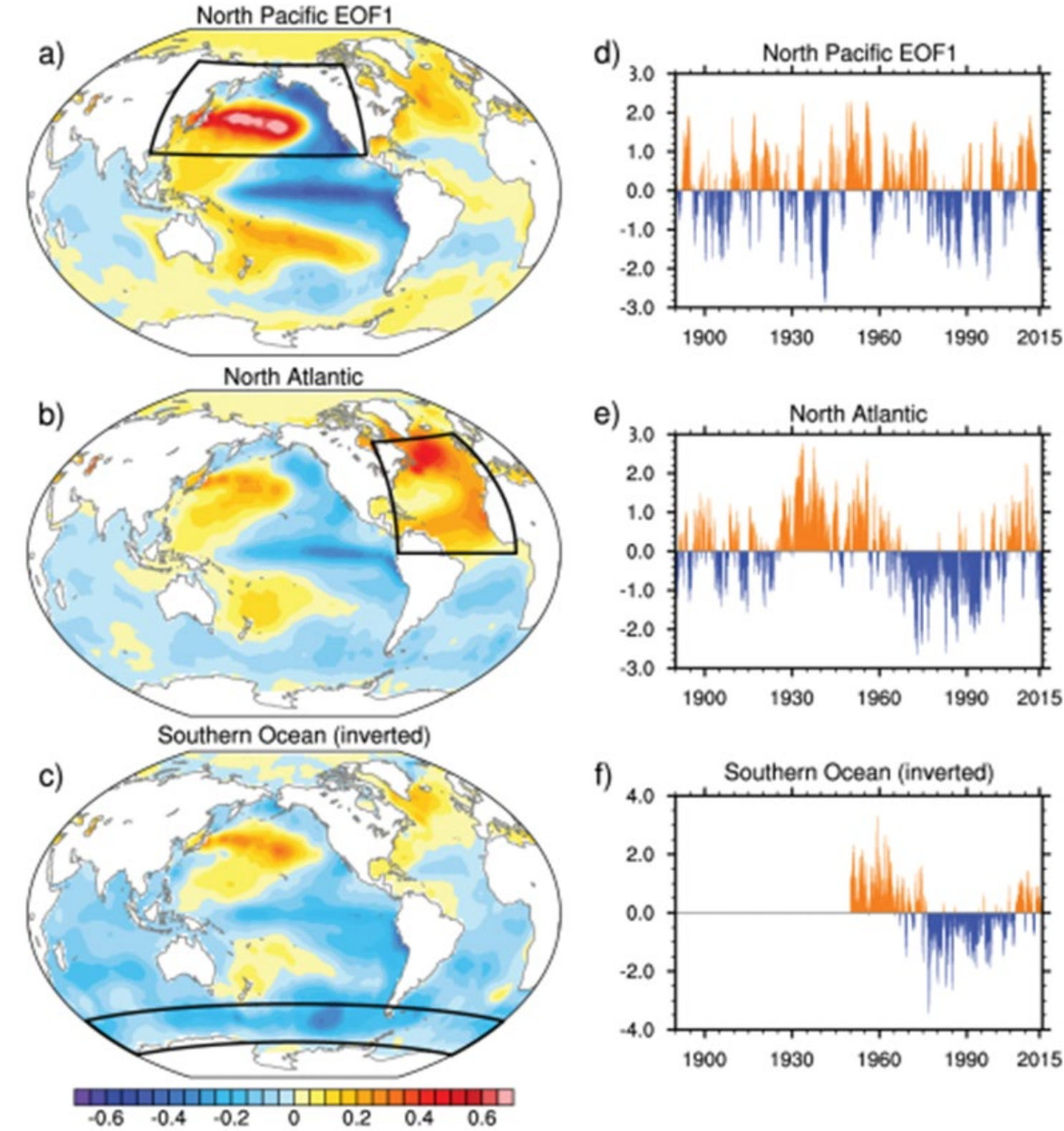


Figure 1: Deser and Phillips (2017) Figure 2; Spatial patterns of EOF-1 (a, b, c) and PCs (e, f, g) based on regional data subsets (black box)

Results

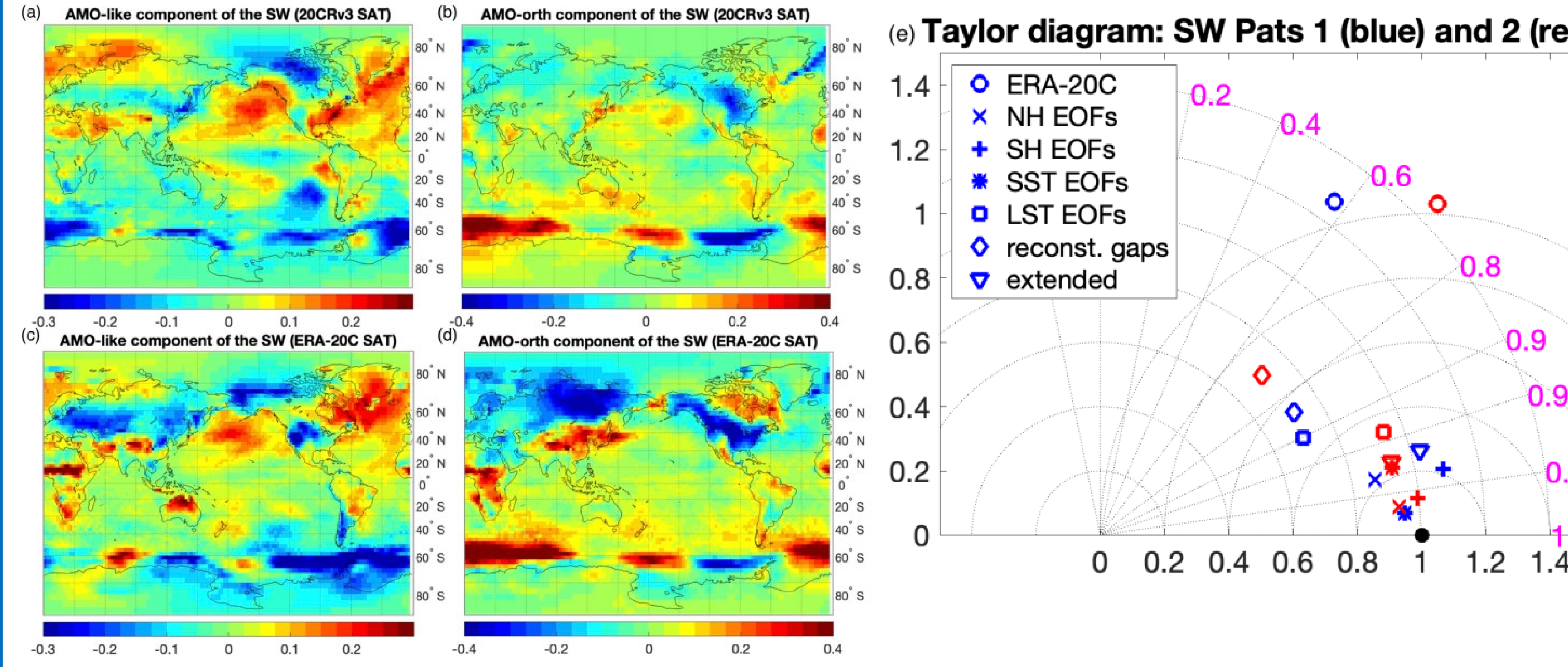


Figure 4: Spatial plots showing (a, c) the first and (c, d) second EOF patterns projected onto (a, b) 20CRv3 and (c, d) ERA20C SAT data. (e) Taylor diagram for patterns 1 (blue) and 2 (red) for ERA20C and 20CRv3 with EOFs based on selected regions, artificial data holes that were then filled, and extended timeseries

- Perform an ensemble EOF analysis on M-SSA-filtered data MCV anomalies and rotate the leading EOFs so that rotated PC-1 is most correlated with AMO and PC-2 lags PC-1 in time
- AMO-like patterns (Figs. 4a,c) match Deser and Phillips over the oceans with exclusion of SO
- MCV includes the 2nd lagged AMO-orth pattern describing the “propagation” of the multidecadal signal (Figs. 4b,d)
- Patterns in relative agreement with each other between two reanalysis datasets (Figs. 4a,b and c,d)
- The above analyses were repeated using 1) using regional, instead of global M-SSA analysis; 2) reanalysis data with original data gaps reintroduced and filled using covariance-based imputation techniques; and 3) extended reanalysis time series, extrapolated into the future and the past using linear inverse models, to gauge the sensitivity of the analysis to the ends
- The similarities between the patterns stemming from the regional and global MCV signal (Taylor diagrams in Fig. 4e and ensemble-mean time series in Fig. 5a,b) indicates the true global teleconnectivity of the MCV
- Reconstructed gaps do not impede the MCV signal detection, shown by the reconstructed gaps diamonds; this is consistent, again, with the global teleconnectivity of the MCV signal

Signal Isolation and detection

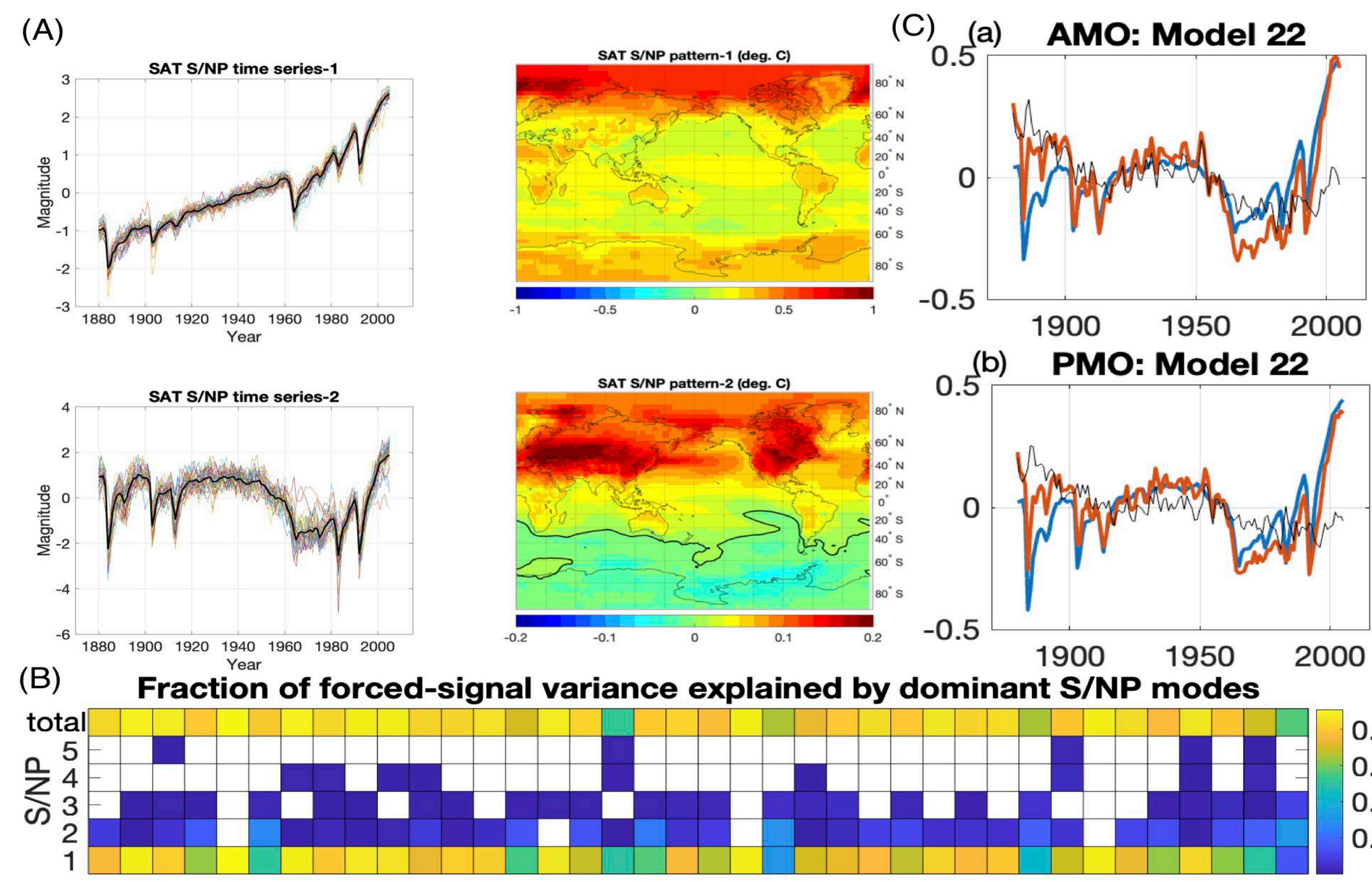


Figure 2: (A) Timeseries of observed forced signal (left column) and ensemble average (right column) of pattern 1 (top row) and pattern 2 (bottom row) projected onto SAT grid data, (B) Fraction of forced signal variance explained by S/NP modes for each forced signal estimate, and (C) AMO and PMO index forced-signal in model 22 with the full estimated signal (red), reconstruction by S/NPs 1-5 (blue) and the difference (black).

- Utilize ensembles from 38 CMIP5/6 models to estimate the forced signal
 - Ensemble mean tends to cancel out internal variability, leaving forced signal
 - Truncated expansion into signal-to-noise (S/NP) maximizing patterns (Wills et al. 2020) instead of the raw data allows one to better isolate the forced signal patterns in small ensembles
- Subtract the forced signal(s) estimated from reanalysis / climate model data to obtain **estimates of internal variability**
- Identify dominant variability in observations and models using multichannel singular spectrum analysis (M-SSA: Ghil et al. 2002)
- Result: optimally filtered MCV signal in observed and simulated climate estimates**
- Reanalyses spectra dominated by leading pair
- Less variance and less separation from the leading pair in model data
- Projection of simulated signal onto reanalysis EOFs shows negligible variances indicating that the observed signal is muted in simulations

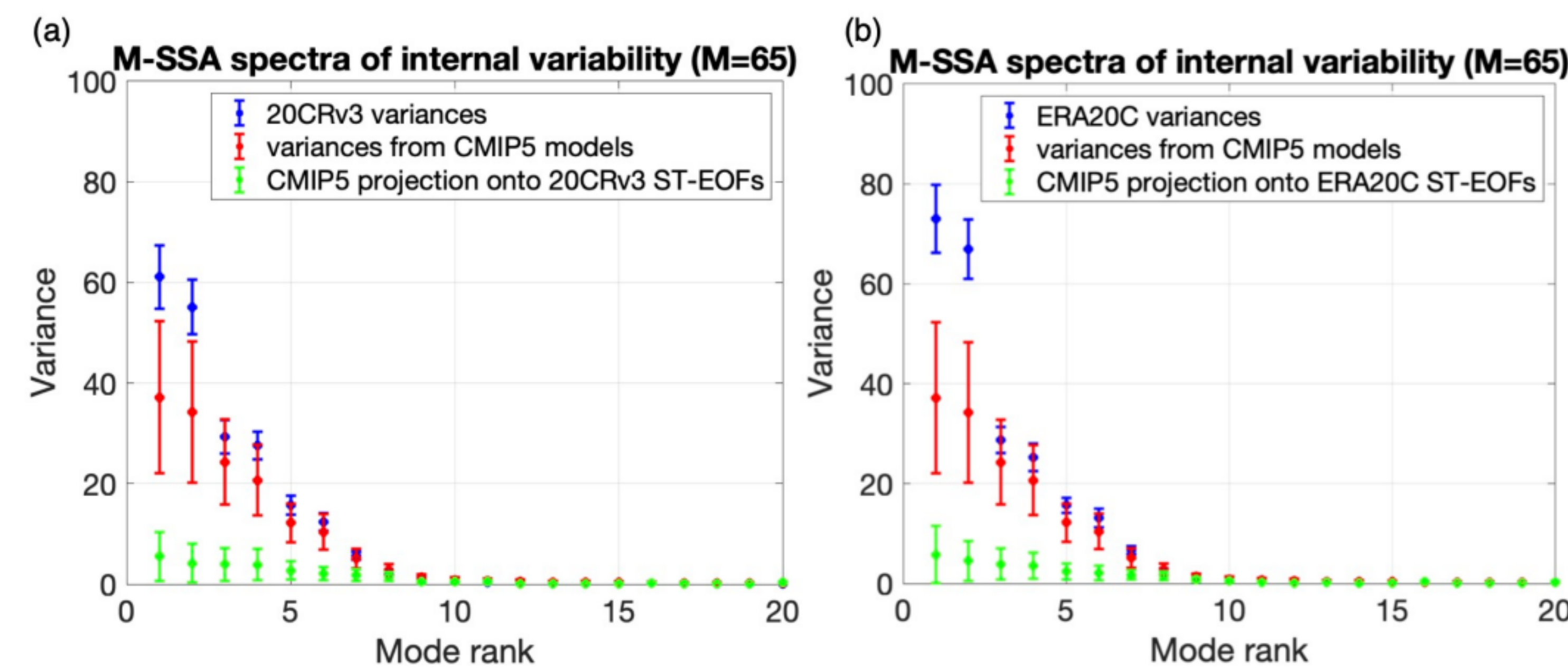


Figure 3: Variance plots showing space-time variance of (a) 20CRv3, (b) ERA20C, and (a,b) CMIP5

- Use S/NP analysis to both identify forced signals in the individual-model ensembles and to analyze the spread of the forced signals estimated in the 38 forced-signal estimates (Fig. 2A)
- The common part of the estimated forced-signal evolution is dominated by S/NPs 1-3 (1 and 2 shown in Fig. 2A) and explains 80% of the forced-signal variance across the forced signal ensemble (Fig. 2B)
- The remaining 20% are due to individual responses specific to each model. Forced-signal responses of some models are substantially different from the forced-signal evolution common in the ensemble and exhibits anomalous responses on multidecadal time scale characterized by apparent global “teleconnections” (Fig. 2C)
- This is one possible reason for observed globally-connected MCV**

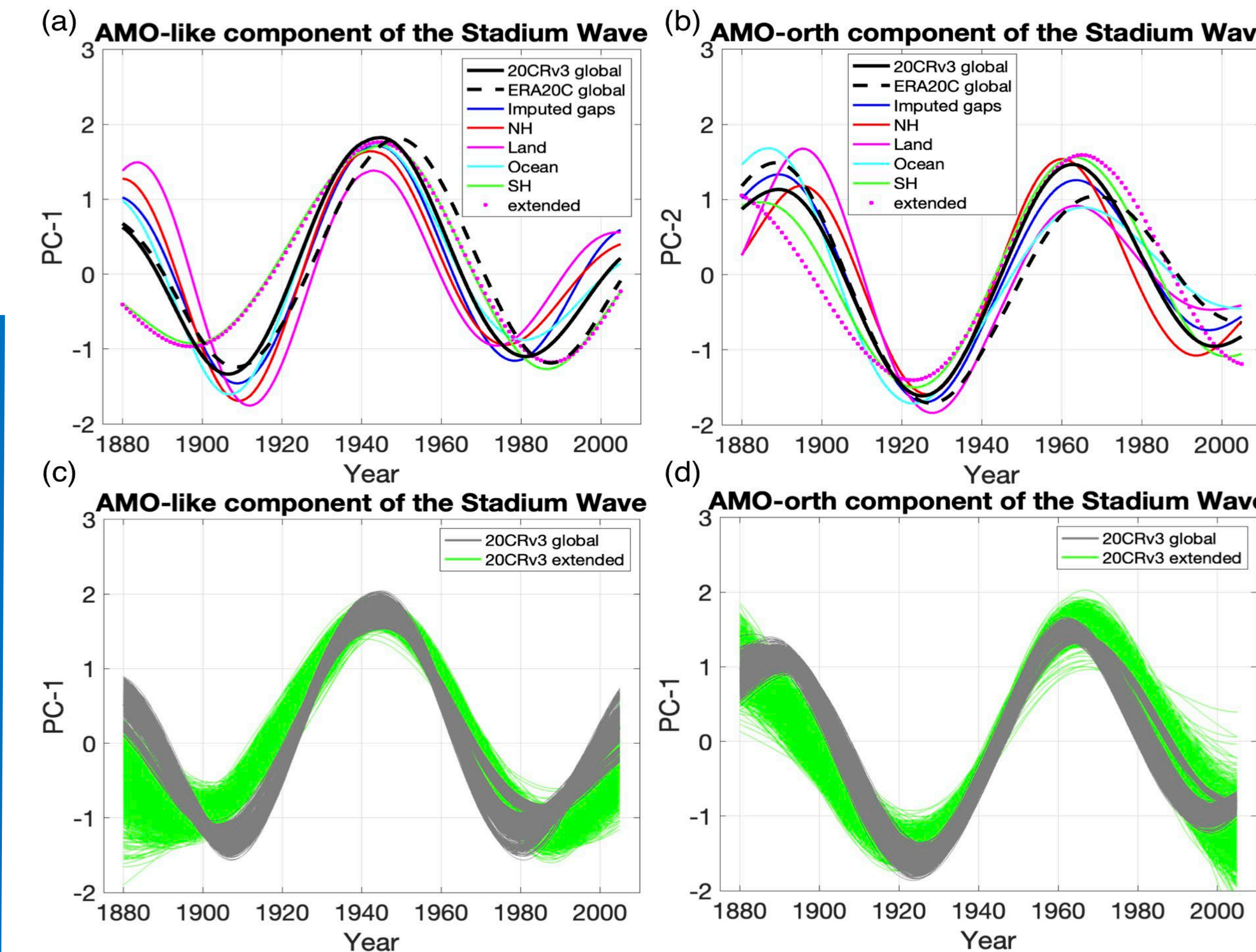


Figure 5: Ensemble-mean time series showing the evolution of (a) AMO-like and (b) AMO-orth patterns estimated using different versions of our analysis (see above); (c, d) the same as in (a, b) but for all ensemble members using 20CRv3 global and time-extended analyses.

- Ensemble-mean timeseries describing the evolution of AMO-like and AMO-orth components of MCV (Fig. 5) show agreement between the different versions of analysis (global vs. regional, the one with imputed data gaps, and the one based on the extended timeseries)
- The largest differences in the evolution occur between the original MCV reconstruction and the one based on time-extended data (Figs. 5c,d)
- Still, the same overall multidecadal evolution is easily identifiable in both time series

Conclusions:

- A distinct multidecadal signal in the reanalysis variability was robustly detected despite the short observational period and sparse data coverage early in the timeseries
- Leading component has the spatial pattern similar to that in Deser and Phillips (2017)
- An equally important second component in quadrature with the first one leads to a propagating signal
- Agreement between regional and global MCV signals indicates true global teleconnectivity of the observed MCV; the identification of this signal is not susceptible to uncertainties associated with missing data and end effects
- The lack of this signal in CMIP simulations may be due to the models misrepresenting either **climate response to external forcings** or **internal climate variability**

References:

Deser, C., and A. Phillips, 2017: An overview of decadal-scale sea surface temperature variability in the observational record. *Past Global Changes Mag.*
 Ghil, M. & Coauthors, 2002: Advanced spectral methods for climatic time series. *Rev. Geophys.*
 Kravtsov, S., C. Grimm, and S. Gu, 2018. Global-scale multidecadal variability missing in state-of-the-art climate models. *npj Climate Atmos. Sci.*
 Wills, R.C.J., D.S. Battisti, K.C. Armour, T. Schneider, C. Deser, 2020. Pattern Recognition Methods to Separate Forced Responses from Internal Variability in Model Ensembles and Observations. *J. Climate*